

Pressure dependent mode transition in an electron cyclotron resonance plasma discharge

Ane Aanesland^{a)} and Åshild Fredriksen^{b)}
Physics Department, University of Tromsø, N-9037 Tromsø, Norway

(Received 13 November 2000; accepted 29 May 2001)

Despite the wide range of applications of the electron cyclotron resonance (ECR) plasma sources, the ECR plasma processing control is tricky at certain operation parameters. There are several reports of regimes where abrupt changes and instabilities in plasma parameters occur. In the present work we report extensive probe measurements of plasma potential, electron temperature, ion beam energy, and velocity as well as plasma density over a mode change appearing when the neutral argon gas pressure is changed. The parameters were measured over the entire pressure range from 0.15 to 7 mTorr. We found a large drop in electron temperature and plasma potential when the pressure increased from 0.15 to 0.4 mTorr. At 0.4 mTorr the temperature reached a minimum and the density a local maximum, while at 1 mTorr the density reached a minimum. When increasing the pressure above 1.2 mTorr the temperature decreased and the density increased rapidly. While the plasma appearance at low and high pressure can be explained by a global conservation model, the behavior in the intermediate pressure between 0.4 and 1.2 mTorr needs a deeper investigation. We discuss the possibility that the mode change is connected to the competition between stepwise and direct ionization of neutral argon and excitations to metastable argon atoms. © 2001 American Vacuum Society. [DOI: 10.1116/1.1387053]

I. INTRODUCTION

Plasma sources based on the electron cyclotron resonance (ECR) are widely used in plasma processing applications.^{1,2} However, at certain control parameters the ECR plasmas display sudden changes in the plasma parameters, resulting in bistable plasma modes and hysteresis.

The ion density is found by some authors to exhibit a hysteresis as the microwave input power is increased and then decreased.³⁻⁶ They all find that at certain levels of input power the ion density increases discontinuously from a low-density to a high-density mode when the power is increased. When the power is decreased, the ion density falls back into the low-density mode but at a lower input power level. Although the qualitative behavior is the same in argon^{4,5} as in nitrogen,⁶ the actual power level at which the transitions occur is different from case to case.

In the cases of mode transitions as a function of pressure, there are no reports of hysteresis. The mode changes are observed as a sudden decrease in floating potential, ion saturation current, and heat flux^{5,7,8} together with increased fluctuations and instabilities at the transition pressure.^{5,9} Hence, the earlier mentioned works indicate that slightly different phenomenology exists for the cases with power variation and pressure variation.

No unanimous conclusions have yet been drawn regarding the nature of these transitions. By most authors they are explained as resulting from the wave propagation in the plasma.^{3,4,8,10} The left-hand polarized (LHP) wave has no direct resonance at the electron cyclotron frequency and, depending on the plasma density, may or may not be able to

propagate in the plasma. Mode changes in the plasma appearance, i.e., density,⁴ radial profile, and light intensity,⁸ have been reported with simultaneous measurements of microwave field intensity. It was found that the microwave intensity was more than three orders of magnitude higher in the downstream area at low density, which is in agreement with the assumption that LHP waves are not effectively absorbed in this mode.

Some authors^{7,5} found that by keeping the ratio of pressure over the wall lining temperature constant, the discontinuous changes in floating potential were avoided. Hence, they concluded that the neutral density, and not the pressure, was the primary parameter governing the mode change.

It has also been reported⁹ that the mode change was suppressed with the introduction of silane to a nitrogen plasma, and that the instabilities and mode changes were dependent on chamber history.

There are no investigations on the full range of plasma parameters in the transition regions. As mostly ion saturation currents, floating potentials and in one case ion energies are reported there is a lack of knowledge on the behavior of the plasma parameters in these transition regions. In this article we report measurements of the full set of plasma parameters in a mode transition arising in an ECR plasma with argon pressure variation. We report the changes in electron temperature, plasma potential, as well as ion densities and ion beam energies in the entire transition region. We suggest that the competition between excitation, stepwise- and direct-ionization processes may play an important role in the mode change.

The article is organized as follows. In Sec. II, we describe the experimental setup, diagnostics, and analysis techniques. In Sec. III, the results are presented and discussed, and the

^{a)}Electronic mail: ane@phys.uit.no

^{b)}Electronic mail: ashild@phys.uit.no

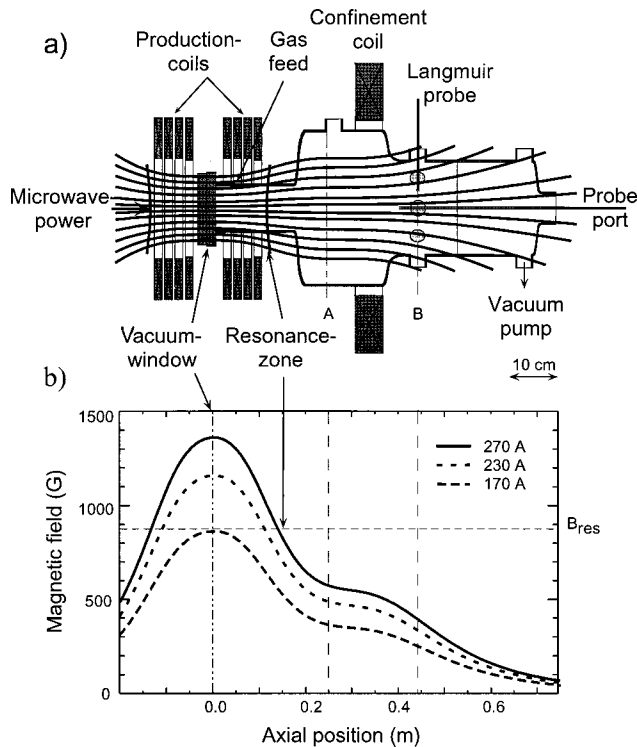


FIG. 1. ECR device with magnetic field configuration. (a) Vacuum chamber, production, and confinement coil arrangement. Magnetic field lines at 270 A coil-current are plotted. (b) Magnetic field strength along the axis of the chamber at four different coil currents. The horizontal line is the resonance value of 875 G, and the leftmost vertical line is the position of the vacuum window. The second and third vertical lines indicate probe port positions.

conclusions with suggestions for future research are given in Sec. IV.

II. EXPERIMENT

The ECR plasma source, “Menja,” has been described elsewhere,¹¹ and the source is shown in Fig. 1(a). The ECR plasma chamber is a cylindrical stainless steel vacuum chamber with a total length of 0.85 m. It is divided into three main parts defined by the chamber circumference where the production part with the resonance zone has the smallest diameter, followed by the downstream, and the process part as shown in the figure.

Microwaves are produced by an Astex A-5000 microwave power generator, which delivered power of 500 W at a frequency of $f_0 = 2.45$ GHz. The waves are converted from a rectangular TE_{10} to a cylindrical TE_{11} mode, and then fed into the chamber via a 7-mm-thick quartz window of 98 mm diameter.

Two sets of four coils supply the resonant magnetic field in a divergent field configuration, while one extra coil provides improved plasma confinement. The microwave introduction window is placed at the maximum of the magnetic field to protect the window from damage due to sputtering. The microwaves propagate through a decreasing magnetic field until they are absorbed by the resonance at the electron cyclotron frequency $\omega_{ce} = eB/m_e$. Here e is the elementary charge, B is the magnetic field strength, and m_e is the elec-

tron mass. The magnetic field at the EC resonance, $\omega = 2\pi f_0 = \omega_{ce}$, is $B_{ce} = 875$ G. The position of the resonance is set by the coil current, and can be located between the microwave window and the end of the production part as shown in Fig. 1(b).

The downstream and process parts of the chamber have ports for diagnostics, pressure monitoring, and pumping. Argon gas is inserted through an inlet close to the microwave window, and the gas flow is controlled by a manually operated needle valve. The chamber is pumped at 501 s^{-1} with a turbomolecular pump placed at the downstream end of the plasma chamber. The radial cross section can be scanned at ports located at 0.27 and 0.45 m from the microwave window. A port at the downstream end from the window was used for axial measurements. In this work we use measurements carried out in the axial center 0.45 m from the microwave window, as well as some data from axial scans between 0.22 and 0.46 m.

A Langmuir probe was used to derive the plasma potential V_p , electron temperature T_e , and electron and ion densities n_e and n_i . The probe was a plane circular tungsten probe with 2 mm diameter and with its plane perpendicular to the magnetic field. The probe signals were digitized by a Tectronix 2430 8-bit digital oscilloscope at 5 kHz sampling rate.

By sweeping the probe potential V_p from -30 to $+30$ V at a sweep rate of 33 Hz, the current-voltage ($I-V$) characteristics were obtained, providing V_p , T_e , and n_e by means of an analysis program utilizing the standard probe theory for nonmagnetized plasmas. This method is taken to give reliable results for V_p and T_e also at moderate magnetic fields.¹²

However, as the magnetic field is about 450 G at the measurement position, the electron Larmor radius r_{Le} is typically about 0.1 mm for 5 eV electrons and the probe radius r_p is much larger than r_{Le} . Hence, the electrons are magnetized and the electron saturation current is depleted, so that the actual electron density is much larger than derived from this current. Since the probe radius is large compared also to the Debye length λ_D a quasicollisionless thin sheath theory is appropriate to estimate the ion density from the ion saturation current, I_+ .¹² This current was extracted by applying a negative direct current bias to the probe and the ion density was derived by means of the Bohm formula for slightly magnetized singly charged ions, given by

$$n_i = 2 \frac{I_+}{eA_s} \left(\frac{T_e}{m_i} \right)^{-1/2}, \quad (1)$$

where the sheath area $A_s \approx A_p$, A_p is the probe area and m_i is the ion mass. The actual bias of the probe was set to -300 V, but the resulting current has been adjusted to match that of a -50 V bias to avoid the effects of sheath expansion. To achieve this, the ion current was multiplied by a factor 0.6 before deriving the density. To calculate the plasma density from Eq. (1) we used the electron temperature measured by the Langmuir probe.

The ion velocity distribution was measured using a gridded ion energy analyzer (IEA). The analyzer consists of an

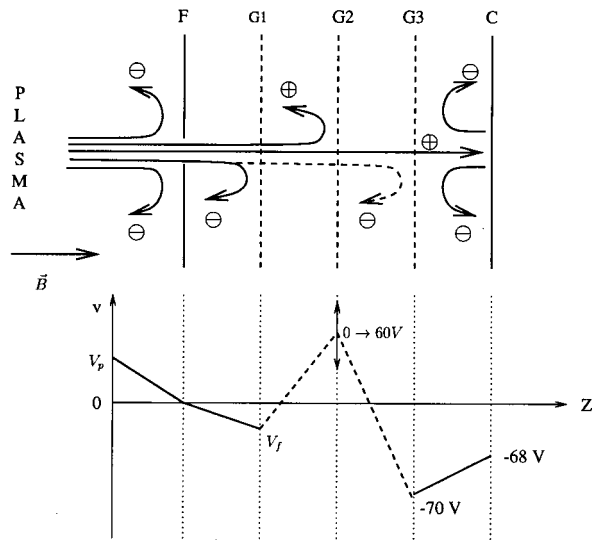


FIG. 2. Potential distribution configuration of the IEA probe.

entrance slit, three grids, and a collector as shown in Fig. 2. The bias on the grids were set in order to obtain a smooth current–voltage characteristics and to minimize the secondary electron effects. The second grid potential, V_g , was swept from 0 to 60 V to obtain the ion velocity distribution. The ion velocity distribution function is proportional to the differential of the measured ion current, I_c , with respect to the grid potential, V_g , given by¹³

$$f(v) = -A \frac{m_i}{e^2} \frac{dI_c(V_g)}{dV_g}, \quad (2)$$

where A is a proportionality constant, and $v = (2eV_g/m_i)$ is the ion velocity. The ion beam energy is defined as the width of the normalized Gaussian velocity distribution at the 1/e point.

Differentiating the I – V characteristic containing noise will increase the noise level in the obtained distribution which becomes distorted and generally lead to an underestimation of the distribution width. If the characteristic is smoothed by some averaging methods before differentiating, the “knee” in the characteristic will be smoothed out as shown in Fig. 3(a). The slope will then be reduced, which will lead to a broadening of the distribution and consequently an overestimation of the beam energy will be the result. Hence, if the characteristic is carefully smoothed so it still contains some noise when differentiating, the under- and overestimation will cancel out, but the distribution will be noisy as shown in Fig. 3(b). In order to find the most correct ion energy distribution and beam energy from the measurements a polynomial of order 10 was fitted to the characteristic, rather than applying a smoothing or averaging procedure. This method gave an excellent fit to the actual characteristics as shown in Fig. 3(a). The polynomial was

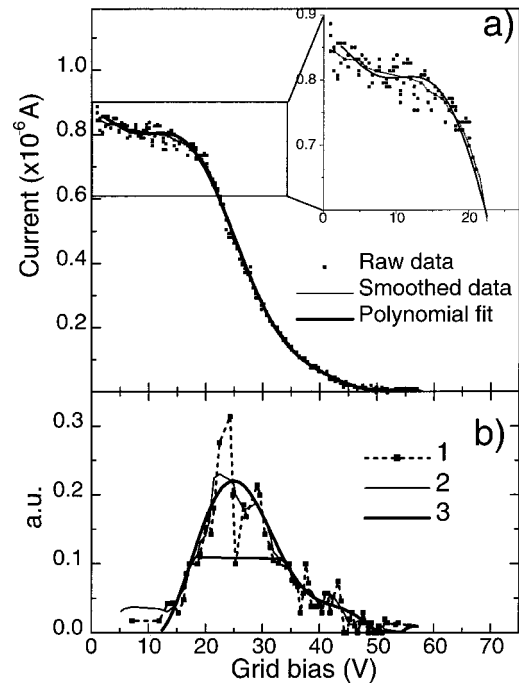


FIG. 3. (a) I – V characteristic measured by the IEA probe, the polynomial curve fit, and the smoothed curve. (b) Ion energy distribution obtained from the smoothed curve (1), smoothed again (2), and the polynomial (3) which is fitted with a Gaussian distribution to find the ion beam energy.

then differentiated numerically over the energy range to obtain the ion distribution, and the ion beam energy was in turn derived from a Gaussian fit to the ion velocity distribution as shown in Fig. 3(b).

III. RESULTS AND DISCUSSION

The electron temperature, T_e , and plasma potential, V_p , derived from the Langmuir probe are shown as a function of pressure in Figs. 4(a) and 4(b), respectively. At the lowest pressure, 0.15 mTorr, the electron temperature is about 6 eV. When the pressure increases T_e drops abruptly reaching a minimum of 2 eV at 0.4 mTorr. With further increase in pressure T_e rises to 4.5 eV at 2.3 mTorr and then decreases slowly with increasing pressure.

The plasma potential decreases from its highest value of 50 V at 0.15 mTorr down to 30 V at 0.4 mTorr. From the transition pressure at 0.4 mTorr, marked by the vertical line in Fig. 4, the plasma potential still decreases, but at a much smaller rate. Around 2.3 mTorr, where the electron temperature reaches a local maximum, the plasma potential shifts to a lower value and then decreases still further at the same rate.

In Fig. 4(c) the plasma density from the ion saturation current measurement is plotted. The plasma density has a local maximum $> 2 \times 10^{17} \text{ m}^{-3}$ at the transition pressure, and then it reaches minimum of $\sim 1.5 \times 10^{17} \text{ m}^{-3}$, at a pressure slightly higher than for the T_e minimum. At pressures above 2 mTorr the density increases with increasing pressure. No saturation was obtained after a sharp increase from 2×10^{17} to $3.5 \times 10^{17} \text{ m}^{-3}$ within our range of measurements.

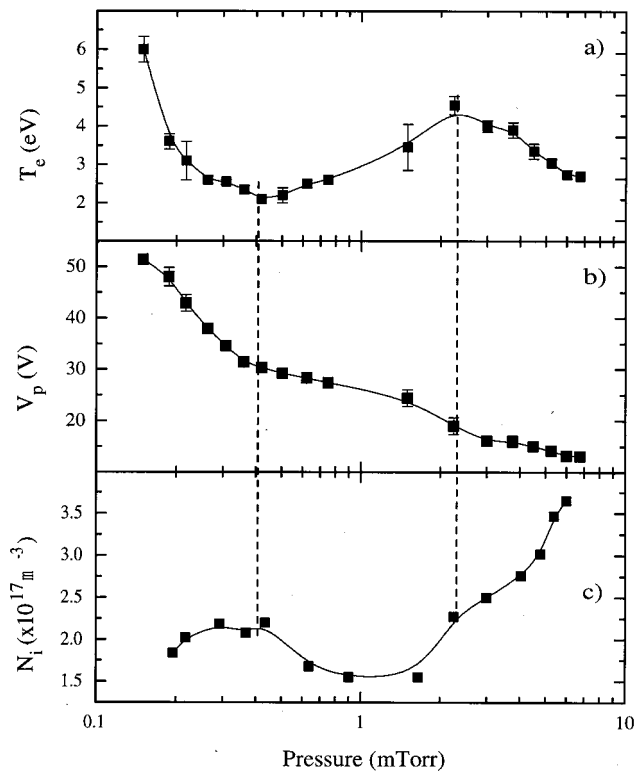


FIG. 4. Electron temperature (a), plasma potential (b), and ion density (c) from Langmuir measurements vs argon neutral pressure.

The error bars of V_p and T_e were obtained by analyzing several I - V characteristics at the same point. The errors in n_i originates from the electron temperature and the ion saturation measurements. By a rough estimate, given 15% error in I_+ we have an estimated error in n_i of 16%–17%.

The results from the ion energy analyzer are shown in Fig. 5. When the pressure is low the ion distribution function has two peaks, with the smallest peak having a high peak velocity and low ion beam energy, but this small peak is not plotted in the figure. As the neutral pressure is increased the peak velocity decreases and the second peak becomes less prominent and vanishes. The beam energy increases with

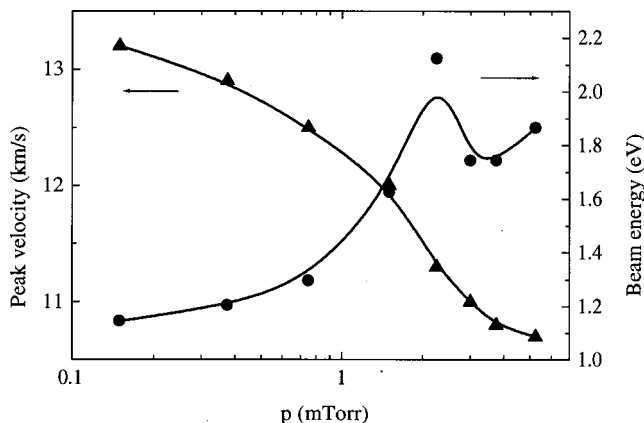


FIG. 5. Ion peak velocity and ion beam energy obtained from the IEA probe.

pressure up to 2.3 mTorr where a local maximum occurs at the same pressure as the T_e maximum.

At the pressure below 0.4 mTorr and above 2 mTorr the plasma parameters changed qualitatively with neutral gas pressure as expected from the literature.^{1,14,15} The rapid drop in the electron temperature at very low pressure, between 0.15 and 0.4 mTorr, can be explained by the nature of the ionization rate coefficient for electron neutral collisions with increasing pressure. The coefficient depends approximately on the electron temperature as¹

$$K_j(T_e) \approx \sigma_j v_e(T_e) \exp\left(-\frac{E_j}{kT_e}\right), \quad (3)$$

where $v_e(T_e) = (8kT_e/\pi m)^{1/2}$ is the mean electron thermal velocity, K_j is the rate coefficient, σ_j is the collision cross section, and E_j is the threshold energy for process j , e.g., ionization or excitation.

In a steady state plasma the global rates of creation and loss of ions are equal, and the balance between the total volume ionization and the loss of particles to the wall, neglecting the recombination of charged particles in the volume, is derived by Lieberman and Lichtenberg¹

$$\frac{K_{iz}(T_e)}{C_s(T_e)} = \frac{1}{n_g d_{\text{eff}}}, \quad (4)$$

where K_{iz} is the rate constant for ionization, C_s is the ion sound speed, n_g is the neutral gas density, and d_{eff} is an estimated effective length of the discharge which depends on the chamber size and the fraction between the bulk and the edge plasma density. Hence, when the neutral gas density is increased by increasing the pressure, the ionization rate coefficient must decrease to maintain the particle balance, which requires a decrease in the electron temperature. From Eqs. (3) and (4) it is evident that T_e is more sensitive to changes in n_g at lower pressure and therefore decreases faster when increasing the pressure in this region. The change in the plasma density is correlated with the change in the electron temperature and ion impact energy.¹⁵ The reason for the low ion density at very low pressure may be due to the fact that the ionization efficiency of the source drops. Since the temperature is so high at this pressure a large fraction of the input power will go to maintain the plasma potential and drive ions to the walls, and less power is left for ionization.

For the pressure above 2 mTorr the same arguments as given earlier are valid. For very high pressure the plasma density is expected to reach a saturation, owing to the decrease in the ionization rate since the electron temperature decreases below the threshold energy for ionization. Also the radial plasma losses will increase via collisions with neutral particles which also participate to reach a density saturation.¹⁶ The plasma was difficult to ignite at the highest pressures above 7 mTorr, and therefore data was not obtained at pressures where density saturation is believed to take place.

A trend of decreasing T_e and increasing n_e with pressure has been observed in several experiments^{8,16,17} and also ob-

tained by modeling and simulations.^{15,18} At the intermediate pressure range between 0.4 and 2 mTorr the plasma parameters were not as expected from the theory. This phenomena is not unique and is observed in several experiments, but not yet obtained in simulations.

The microwaves that are introduced into the plasma chamber are plane linearly polarized waves. They can be represented as a superposition of a right- and left-hand-polarized wave, RHP and LHP waves respectively. The RHP waves will be effectively absorbed at the ECR position, but the LHP waves are not directly absorbed at this resonance. These waves will either propagate downstream to lower magnetic field or be reflected back when reaching a threshold plasma density, i.e., the cutoff density.

The cutoff density for the LHP wave in a magnetized plasma where $B > B_{ec}$, is given by^{19,10}

$$n_c = n_{c0} \left(1 + \frac{\omega_B}{\omega} \right) = n_{c0} \left(1 + \frac{B}{B_{ce}} \right). \quad (5)$$

$\omega_B = eB/m_e$ is the electron cyclotron frequency at the magnetic field B . n_{c0} is the cutoff density for the LHP wave in an unmagnetized plasma where the wave frequency is equal to the plasma frequency, and is given as

$$n_{c0} = \frac{m_e \epsilon_0 \omega^2}{e^2}, \quad (6)$$

where ω is the wave frequency, and ϵ_0 is the permittivity in vacuum. Using the microwave frequency $f_0 = 2.45$ GHz, the cutoff density at zero magnetic field is $n_{c0} = 7.45 \times 10^{16} \text{ m}^{-3}$. The LHP-cutoff density at the ECR position is $n_c = 2n_{c0} = 1.5 \times 10^{17} \text{ m}^{-3}$, while $n_c = 2.6n_{c0} = 1.9 \times 10^{17} \text{ m}^{-3}$ at the microwave window where $B = 1400$ G. The LHP wave propagates downstream at densities below n_c , whereas at higher densities it is reflected back to the microwave generator, or it transforms to longitudinal plasma waves or RHP waves in the region where $n_e \approx n_c$.^{4,10} Hence, in the case where the LHP wave propagates in the underdense regime it will carry away some of the power, which in the overdense regime is effectively absorbed in the resonance zone. Consequently the ionization is less efficient and the plasma density will remain smaller than the cutoff density. The net microwave power has been measured downstream in a mirror field ECR plasma source.⁸ A microwave power increase by three orders of magnitude in the pressure range between 0.13 and 2.8 mTorr, was measured where they simultaneously observed an underdense mode. It is also reported elsewhere that below the critical density there is a state where the plasma is nearly transparent to microwaves, which results in standing waves within the chamber due to reflections.⁴ These results compared with our results seem to indicate that the sudden change in our plasma parameters might be a transition from an underdense $n_e < n_c$ to an overdense mode $n_e > n_c$.

However, during the gas breakdown, before steady state is obtained there will be a short time where the plasma density is low and the LHP wave is able to propagate in the plasma chamber. When the plasma reaches the steady state some

mechanism must “decide” if the plasma density stays below or grows above the cutoff density. Since the LHP wave is initially able to propagate in the plasma it is reasonable to believe that the propagation or cutoff of this wave is not the mechanism responsible for our mode change, but is an effect of this mode change.

There are also several reports that are inconsistent with the wave-cutoff theory. Aydil *et al.*⁵ and Jarnyk *et al.*⁷ report mode changes similar to ours, where the plasma density was sometimes about ten times larger than the cutoff density both before and after the transition, and additionally the authors observed a mode change at two distinct pressures and consequently two different densities. Mode changes where the plasma densities were too low for the LHP cutoff to occur are also published.²⁰

In our experiment the plasma density was measured downstream at about 30 cm from the resonance zone. Given the conservation of the magnetic flux along the chamber axis, the relation between the measured density and the density in the resonance zone is

$$n_{res} = \frac{B_{res}}{B} n, \quad (7)$$

where B_{res} and B are the magnetic field strengths in the resonance and measured position, respectively. Here we assume that the charged particles moving along the magnetic field lines are adiabatic, the ion velocity in the resonance zone and downstream are approximately equal, and that the downstream production of charged particles is neglected. In the probe position the magnetic field is 450 G so that the plasma density in the resonance is estimated to be about twice as large as the measured density. In Fig. 6 are shown ion densities measured as a function of distance from the microwave window at two different pressures, one just below the mini-

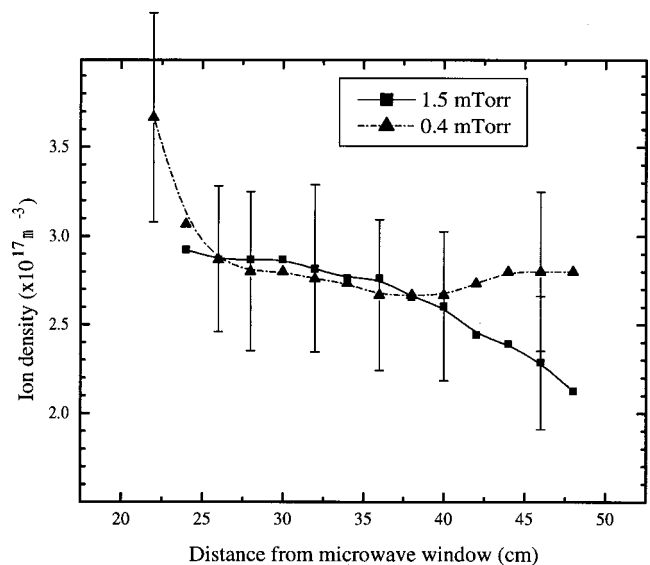


Fig. 6. Profiles of the ion density as a function of distance from the microwave window, at 0.4 and 1.5 mTorr neutral gas pressure and coil current 270 A. Some typical error bars are shown.

imum density pressure (0.4 mTorr) and the other within the density minimum at 1.5 mTorr. The data at 1.5 mTorr shows slightly higher values at 45 cm than the data set of Fig. 4. This might be due to some inaccuracy in the pressure reading, as this pressure is close to the transition where the density increases rapidly with pressure. The position closest to the window (22 cm) corresponds to the region at the bottom end of the steepest part of the magnetic field gradient shown in Fig. 1(b), where the field strength is about 600 G. At this point the densities have increased by 30%–40% relative to the densities at 45 cm. This indicates that the density at the resonance is indeed 1.9–2 times higher than measured 45 cm from the window, in agreement with the estimate before.

The mean plasma density depends primarily on the power deposited in the plasma. Since we keep the microwave power constant, at 500 W, the changes in the plasma density is in our case a consequence of the change in either the electron temperature or the neutral gas density, or both. Jarnyk *et al.*⁷ suggested that the neutral gas density is responsible for the mode change. They showed that by controlling the neutral density, which was done by controlling the ratio between the pressure and the neutral gas temperature, the mode change was avoided. When the same experiment was done by a pressure control only, a mode change occurred. The neutral gas temperature increased from 295 to 343 K after 5–10 min. Hence, when the experiment was controlled by the pressure the density, using ideal gas law, would increase with a factor 1.16. Using Eq. (4) we see that the ionization rate constant will fall with the same factor, and from Eq. (3) it follows that the electron temperature will decrease, but insignificantly. As we observe in the mode change the electron temperature falls, and the result of Jarnyk *et al.*⁷ shows that the floating potential falls in the mode change, but the effect of the neutral gas heating is probably insignificant for our phenomena. According to some authors⁶ the mode transition occurs at essentially the same microwave power at several pressures, which also shows disagreement with the neutral gas heating assumption. We also observe that the mode change occurs both when going down and up in pressure continuously without turning off the plasma which indicates that gas heating is insignificant in our case.

In the intermediate pressure range the electron temperature increases with neutral gas density, which is in contradiction with Eq. (4) where we expect the temperature to decrease with neutral density, as observed at lower and higher pressures. This increase in T_e is not yet understood. Equation (4) is found from the balance between the creation and loss of ions. Hence, some of the assumptions made in deriving this equation fail in this pressure range, and the particle balance equation is probably more complex. A global model of high density argon plasma where the time evolution of the electron temperature and the plasma density are calculated by solving the particle and energy balance equation, with several different reactions considered, has been developed by Ashida *et al.*²¹ This model shows that about 16% of the ionization takes place from the $4s$ and $4p$ excited states at an

electron temperature of about 3 eV, and hence, the contribution of excited states to the entire ionization process is not negligible. Comparing the rate constants for direct and stepwise ionization, i.e., ionization through an excited state, given in Ref. 22 shows that the stepwise ionization is more important at lower electron temperatures <5 eV. The rate constants for electron-neutral collisions which create ions from the ground state and excitation to a metastable state as a function of electron temperature are shown in Wu *et al.*,¹⁵ and the expressions can be found in other references as well.^{1,21,22} It was shown that at temperatures less than 3 eV the production of metastable atoms has a higher rate than the production of ions by the direct ionization process, and at temperatures higher than 3 eV the direct ionization process rate is the largest of these two processes. Thus, the observations indicate that when the electron temperature falls below about 3 eV a larger fraction of the input power goes to production of metastable atoms in either the $4s$ or $4p$ state, which may result in a lower and almost constant ion density in this pressure range. The full investigation of the different processes as a function of temperature and pressure is out of the scope of this article, but it is likely that the explanation for the anomalous behavior occurring in the intermediate pressure lies in the nature of the criteria for different reactions appearing in the discharge. Hence, we suggest that the production rate of metastable atoms and stepwise ionization as functions of the electron temperature may be important factors in understanding the observed mode change.

IV. CONCLUSION

A comprehensive investigation of changes in electron temperature, plasma potential, ion density, and ion beam energy as a function of pressure has been reported. The plasma parameters were measured over the entire pressure range from 0.15 to 7 mTorr. We found that for low pressure <0.4 mTorr, and high pressure >2 mTorr the qualitative plasma behavior with neutral gas pressure could be explained by a global conservation model where the creation of ions by direct ionization in the volume is balanced with the loss of particles to the wall.^{1,15} For the intermediate pressure between 0.4 and 2.0 mTorr there was an anomaly in the plasma appearance characterized by a low but increasing electron temperature and a low and almost constant ion density. This anomaly may be explained as a mode change where the production of metastable atoms increases and the ionization becomes less effective.

A more complex model of the particle balance equation as a function of temperature and pressure may be developed where the different processes are taken into account, as done in Ashida *et al.*²¹ for the calculation of the time evolution of T_e and n_i . The mode change will be thoroughly investigated in future work where the neutral gas density, the metastable atom density, and the mass spectra will be investigated, which hopefully will provide more answers to the question why these mode changes occur.

ACKNOWLEDGMENTS

The authors are grateful for useful discussions with G. Hellblom, K. Rypdal, and S. Ratynskaia. Expert technical assistance was provided by K. Sandaker, K. A. Willumstad, and T. Brundtland. This work was made possible by Grant No. 116434/410 from the Norwegian Research Council.

¹M. A. Lieberman and A. J. Lichtenberg, *Principles of Plasma Discharges and Materials Processing* (Wiley, New York, 1994).

²J. Asmussen, T. A. Grotjohn, P. Mak, and M. A. Perrin, *IEEE Trans. Plasma Sci.* **25**, 1196 (1997).

³O. A. Popov, *J. Vac. Sci. Technol. A* **8**, 2909 (1990).

⁴D. A. Carl, M. C. Williamson, M. A. Lieberman, and A. J. Lichtenberg, *J. Vac. Sci. Technol. B* **9**, 339 (1991).

⁵E. S. Aydil, J. A. Gregus, and R. A. Gottscho, *J. Vac. Sci. Technol. A* **11**, 2883 (1993).

⁶Z. Y. Fan and N. Newman, *J. Vac. Sci. Technol. A* **16**, 2132 (1998).

⁷M. A. Jarnyk, J. A. Gregus, E. S. Aydil, and R. A. Gottscho, *Appl. Phys. Lett.* **62**, 2039 (1993).

⁸S. M. Gorbalkin, L. A. Barry, and J. B. Roberto, *J. Vac. Sci. Technol. A* **8**, 2893 (1990).

⁹F. S. Pool, *J. Appl. Phys.* **81**, 2839 (1997).

¹⁰O. A. Popov, *J. Vac. Sci. Technol. A* **9**, 711 (1991).

¹¹Å. Fredriksen, A. Aanesland, G. Hellblom, and K. Rypdal, *ECA* **22C**, 2789 (1998).

¹²I. H. Hutchinson, *Principles of Plasma Diagnostics* (Cambridge University Press, Cambridge, 1987).

¹³C. Böhm and J. Perrin, *Rev. Sci. Instrum.* **64**, 31 (1993).

¹⁴F. F. Chen, *Introduction to Plasma Physics and Controlled Fusion* (Plenum, New York, 1983).

¹⁵H.-M. Wu, D. B. Graves, and R. K. Porteous, *Plasma Sources Sci. Technol.* **4**, 22 (1995).

¹⁶O. A. Popov, S. Y. Shapoval, M. D. Yoder, and A. A. Chumakov, *J. Vac. Sci. Technol. A* **12**, 300 (1994).

¹⁷J. Forster and W. Holber, *J. Vac. Sci. Technol. A* **7**, 899 (1989).

¹⁸R. A. Dandl and E. G. Guest, *J. Vac. Sci. Technol. A* **9**, 3119 (1991).

¹⁹T. H. Stix, *Waves in Plasmas* (AIP, New York, 1992).

²⁰P. K. Shufflebotham and D. J. Thomson, *J. Vac. Sci. Technol. A* **8**, 3713 (1990).

²¹S. Ashida, C. Lee, and M. A. Lieberman, *J. Vac. Sci. Technol. A* **13**, 2498 (1995).

²²B. M. Smirnov, *Physics of Weakly Ionized Gases* (Mir, Moscow, 1981).